



OPEN

The structure and formation of giant Marimo (*Aegagropila linnaei*) in Lake Akan, Japan

Keisuke Nakayama^{1✉}, Katsuaki Komai^{2,7}, Keisuke Ogata¹, Toshiro Yamada³, Yukinobu Sato⁴, Fumiya Sano⁴, Shintarou Horii⁵, Yuichiro Somiya⁵, Etsuko Kumamoto¹ & Yoichi Oyama^{6,7}

Aegagropila linnaei is a freshwater green alga, which at one time was distributed widely in the northern hemisphere. The aggregate often forms beautiful spherical shapes known as “lake balls” or “Marimo”. The population of Marimo has been rapidly decreasing worldwide, and today the large Marimo, with a diameter of more than 12 cm, exist only in Lake Akan in Japan. However, how Marimo grow and maintain their unique spherical shape in natural habitats remains unsolved. Here we show that Marimo are “polished” into spheres by the rotation induced by wind waves. Such a process enhances the water exchange between the interior and exterior of the Marimo, thereby recycling nutrients for growth. Our results provide an intriguing model of a physical environment interacting with biological processes in a self-sustaining ecosystem. We also demonstrate that Marimo have a spherical annual ring structure, and their growth rate is associated with ice cover. The balance between the ecology of Marimo and the water environment in Lake Akan is highly vulnerable and at risk of irreversible degradation. We must endeavor to rescue Marimo from the fate of a “canary in the coal mine” of global climate change.

Aegagropila linnaei is a freshwater green alga^{1,2}, which at one time was distributed widely around the northern hemisphere¹. *A. linnaei* has a branched filamentous form and grows as attached, floating unattached, and aggregated growth forms^{3,4}. The aggregate often forms beautiful spherical shapes known as “lake balls”, “*Cladophora* balls”, or “Marimo (in Japanese)”, which reach a size of over 20 cm in diameter^{3–5} (Fig. 1a). *A. linnaei* is thought to grow under multiple environmental factors, such as hydro-meteorological and topographical conditions^{4,5,7,12–14}.

The population of *A. linnaei* has declined worldwide^{6–11}. An investigation of *A. linnaei* in the Netherlands concluded that the species had disappeared in all regions of that country due to eutrophication⁹, and another study reported that large Marimo (10–12 cm in diameter or more) were found only in Lake Mývatn in Iceland and Lake Akan in Japan in 2004⁷. The Marimo population in Lake Mývatn started to decline with the increasing algae bloom around the 1990s and almost disappeared entirely in 2013¹¹. Since then, the large Marimo, with a diameter of more than 12 cm, exist in Lake Akan only in the world. Marimo in Lake Akan were designated as a Natural Monument by the Japanese Government in 1921 and a Special Natural Monument in 1952. Nevertheless, two out of the four colonies of Marimo disappeared in the 1940s due to sediment deposition caused by lumber transport using rivers¹⁵. The other two colonies had also been at risk of extinction due to such factors as the water-drawdown cycle of hydropower plants, disturbance of the lake bottom by ships, and eutrophication^{16–19}. Fortunately, these two colonies have been conserved until now and continue to produce giant Marimo (over 20 cm in diameter). An isozyme study showed that the spherical colonies in Lake Akan were genetically homogeneous, implying vulnerability to environmental stressors²⁰. Another study found that Japan was the ancestral area for *A. linnaei* based on internal transcribed spacer (ITS) ribosomal DNA sequences²¹. Thus, Lake Akan is considered the only site with potential for the conservation of *A. linnaei*. However, how Marimo grows and maintains its unique spherical shape in natural habitats remains unsolved. Since the late nineteenth century it has been suggested that Marimo are formed by the rotation induced by wind waves^{5,22–24}, meaning that hydrological studies are needed to clarify Marimo’s formation in the lake. Nonetheless, there have been few studies of the physical characteristics of Marimo and their habitats, because instruments with a sufficient capacity for monitoring underwater dynamics were not widely available before the decline of the Marimo populations worldwide.

¹Graduate School of Engineering, Kobe University, Kobe 657-8501, Japan. ²Faculty of Engineering, Kitami Institute of Technology, Kitami 090-8507, Japan. ³Nishimuragumi Co., Ltd., Yubetsu 099-6404, Japan. ⁴Housui Engineering Consultants Co., LTD., Sapporo 065-0033, Japan. ⁵Center of Radiology and Radiation Oncology, Kobe University Hospital, Kobe, Japan. ⁶Marimo Research Center, Kushiro Board of Education, Kushiro 085-0467, Japan. ⁷These authors contributed equally: Katsuaki Komai and Yoichi Oyama. ✉email: nakayama@phoenix.kobe-u.ac.jp

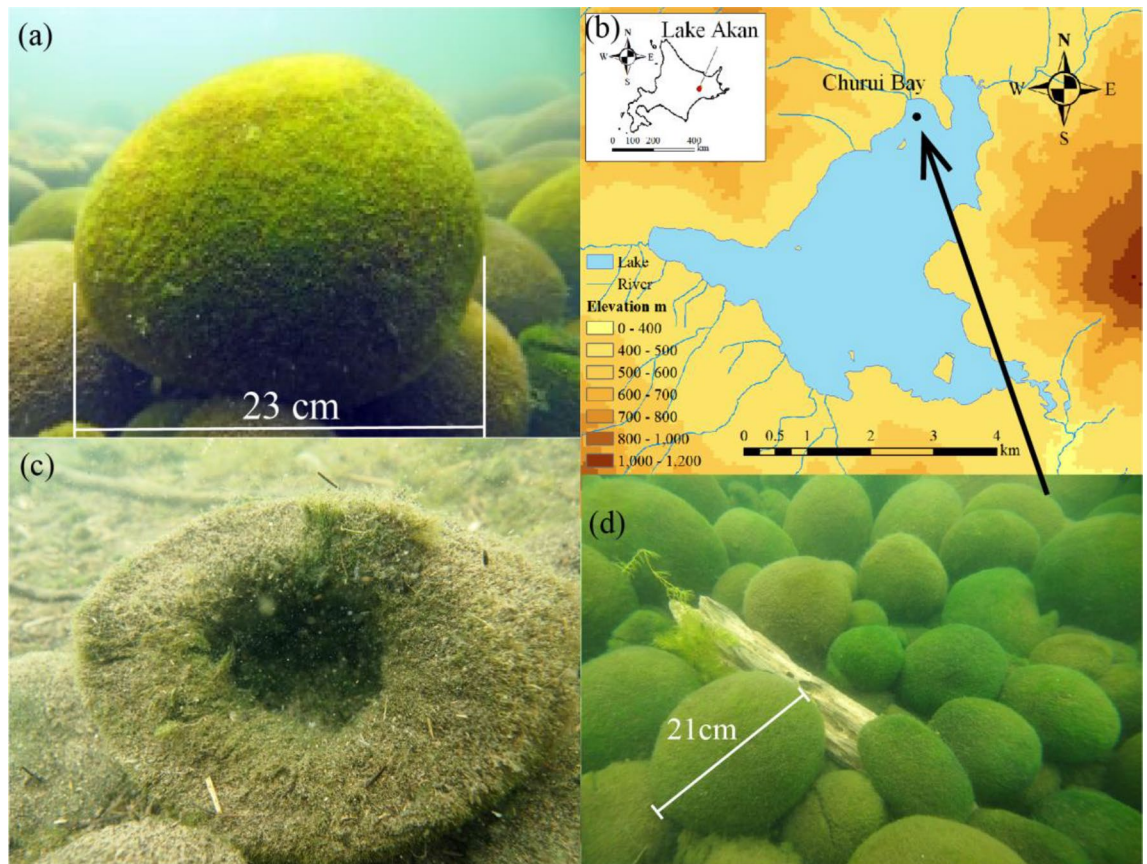


Figure 1. Marimo in Lake Akan. (a) Marimo, (b) Lake Akan and Churui Bay, (c) Collapsed Marimo, (d) Marimo colony in Churui Bay. Map made by ESRI ArcGIS 10.8.

In 2014, the Japan broadcasting corporation took the first underwater footage of the rotation of Marimo in Lake Akan. By analyzing these video images and the accompanying meteorological data, our research team was able to verify that wind waves rotate Marimo^{14,25}. In the six years since those experiments were conducted, further advances have been made in measurement technologies, and the new systems have the potential to provide additional data to unravel the age-old mystery of how Marimo grow and maintain their sizeable spherical shape. In the present study, therefore, we investigated the behavior of Marimo using underwater video cameras, an anemometer, and a wave height meter. First, we revealed the internal structure of Marimo by using magnetic resonance imaging. Second, the physical and meteorological parameters required for the formation of Marimo were obtained. Finally, we revealed that Marimo grow due to the interaction between physical and biological processes in a self-sustaining ecosystem by analyzing the exchange of dissolved oxygen (DO) and nutrients between the interior and exterior of Marimo.

Marimo in Lake Akan. Lake Akan is a caldera lake in the Akan-Mashu National Park of the eastern Hokkaido Island with a surface area of 13.28 km² and depth of 45 m. Marimo grow in Churui Bay and Kinetanpe Bay in the northern portion of Lake Akan (Fig. 1b). Giant Marimo grow in a water depth from 2 to 3 m, and collapsed Marimo and unattached floating mats exist in deeper water. Marimo of a few cm to about 30 cm diameter form layers, with the smallest spheres lying in the bottom layer, and the giant Marimo inhabiting the top layer (Fig. 1a,d). The individual Marimo consist of an aggregation of branched uniseriate green alga filaments and grow by photosynthesis. Marimo of more than 10 cm have a central cavity with a surface thickness of 4–5 cm, which is the approximate depth limit that the *A. linnaei* can exploit for photosynthesis²⁶ (Fig. 1c). In the collapsed Marimo shown in Fig. 1c, fine sediments, including particulate organic matter, cover the surface, suggesting that the Marimo must somehow shake or throw off these deposits by oscillating and rotating in order to sustain its growth by photosynthesis^{14,27}. Note that the collapsed Marimo get into a few cm pieces; still, they survive in the colony and become a giant Marimo though the formation mechanisms remain unsolved.

When the Marimo's diameter becomes greater than 10 cm, a central cavity appears inside due to decomposition, resulting in septic matter accumulation. Thus, the underwater specific density of Marimo becomes smaller with increasing diameter (Figs. 2, 6, 7, 8). For example, the specific density of a 23 cm diameter Marimo sphere is half that of a 16 cm diameter sphere. Marimo with small diameter are likely to drop into gaps in the layered colony structure, resulting in the predominance of large diameter Marimo at the top layer. Therefore, we identified an additional phenomenon occurring in this species: the oscillational motion of wind waves moves the giant

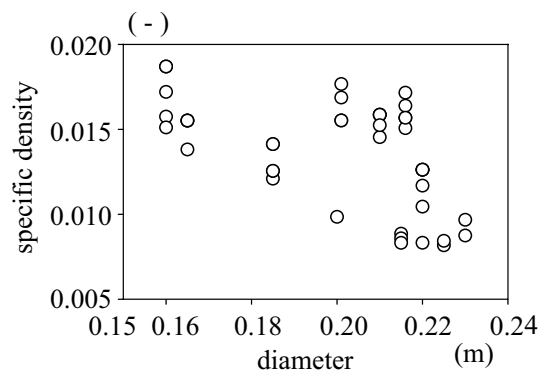


Figure 2. Diameter and underwater specific density of Marimo.

Marimo to the top layer because of their smaller underwater specific density, as shown in Fig. 1a,d. Note that the gas bubbles due to photosynthesis also change the buoyancy of the Marimo²⁸.

Results and discussion

Annual rings of Marimo. We conducted a non-destructive analysis using magnetic resonance imaging (MRI) (Intera Achieva 1.5T Nova Dual; Philips) to investigate the void ratio inside of Marimo (Fig. 3). For MRI analysis of the void ratio, we placed Marimo into a polyethylene bag filled with water. We obtained a proton density-weighted image using Head Coil, which showed that the higher the density of green alga filaments, the larger the MRI value. The black area inside the Marimo sphere indicates the base of the individual Marimo, which is the origin of the Marimo and relocates to the center of the sphere when the Marimo grows sufficiently. We did not observe the base of the Marimo in the center of a 6 cm Marimo, suggesting that it was still growing (Fig. 3a). However, the base is located at the center in a 10 cm Marimo (Fig. 3b). In contrast, the central cavity's MRI values are higher than the other areas when the diameter is more than 16 cm (Fig. 3c–e). The higher central values may correspond to detached organic matter because of the lack of photosynthesis.

All Marimo had annual rings that appeared as sparse and dense patterns. The MRI values were confirmed to be relatively higher adjacent to the Marimo surface than a few mm inside. The MRI analysis was conducted using Marimo sampled in June and July, suggesting that the Marimo surface is highly dense in Spring and Summer compared to other seasons. Indeed, it was shown that spherical colonies might drift into shallow parts with gently sloping sandy bottoms, where, by the intensive rolling motion of the waves⁵. On the other hand, it was revealed that the aggregation of branched uniseriate green alga filaments gradually loosened without any external force and motion for ten years²³. It was also reported that Marimo became bushy in a water tank with no movement²⁹. Admittedly, there is no significant external force during winter because the water surface is entirely covered by more than 0.5 m thick ice. Therefore, the sparse and dense patterns may correspond to the annual change in the surface void ratio of Marimo. We calculated the spectrum using all MRI values along the normal direction to investigate the predominant thickness of the annual rings (Fig. 9). The maximum peak principal thickness was 6.3 mm, and the second peak was 4.5 mm (Fig. 3f).

Rotation of Marimo. Inflow discharge into Churui Bay is about 0.2 m³/s and does not vary widely. Thus, the current induced by inflow is less than a few mm/s, suggesting that the rotation of Marimo is not influenced by an inflow effect. As a major external force, wind blowing over the water surface drives two different motions in a water body; one is the wind-driven current, and the other is the oscillational flow due to wind waves. However, the ice entirely covers the water surface in Lake Akan from December to April. Therefore, wind-driven currents or wind waves are the only factors controlling the oscillation and rotation of Marimo from May to November. It was shown that the wind-driven current washes giant Marimo from a colony to shore in the typhoon event, but does not occur on regular days¹⁹. In contrast, the oscillation due to wind waves is the dominant motion for Marimo on regular days²⁵. They revealed that the fetch at Churui Bay is the longest, 2.5 km when the wind direction is from southeast to southwest, the prevailing wind direction in Lake Akan²⁴. Therefore, even when the wind speed is not so high, such as the wind speed from 5 to 10 m/s, wind waves may induce enough oscillation to rotate Marimo¹⁴. We measured wind speed and wind direction at the height of 2 m above the water surface of Churui Bay in 2014 and 2015 (Fig. 10). The dominant wind cycle was 24 h, corresponding to a typical land and sea breeze in Lake Akan, resulting in a significant wave height of 0.2 m and a period of 1.5 s.

To investigate how Marimo oscillate and rotate in response to wind waves, we recorded their response using an underwater video camera. The video images were recorded in 2014. Adequate wind waves are needed for Marimo to oscillate and rotate. For example, Marimo start rotating when the wind direction is from southeast to southwest. The diameter range was from 15 to 25 cm, and 12 Marimo were selected to investigate the relationship between wind speed and Marimo's rotational angular rate, which provided 52 data plots. First, we attempted to decide the critical wind speed at which Marimo start rotating using the wind speed and video images. 4.8 m/s was found to be the critical wind speed at which the Marimo began to rotate. Then, the average rotational angular rate was modelled as a function of wind speed, $r^2 = 0.65$ ($p < 0.01$) (Fig. 4a). Note that it is needed to conduct

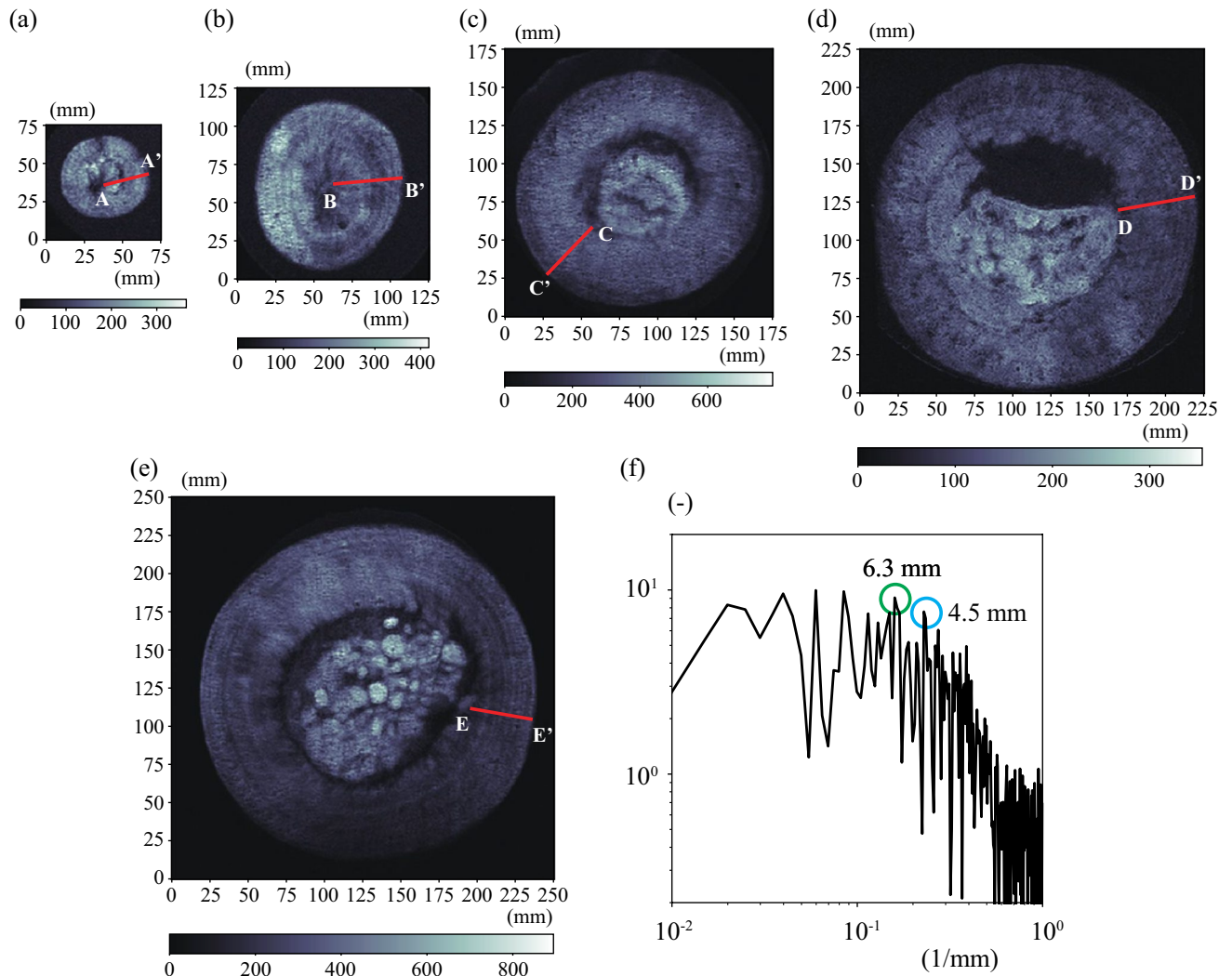


Figure 3. Magnetic resonance images. (a) Diameter of 6.0 cm, (b) Diameter of 10.0 cm, (c) Diameter of 16.0 cm, (d) Diameter of 20.0 cm, (e) Diameter of 22.0 cm, (f) Spectrum of MRI values along red lines.

more field observations and laboratory experiments to model Marimo's rotational angular rate by considering Marimo's diameter and how to overlap in the layers. The critical wind speed may change in a future study, and there is the possibility that the response of Marimo's rotational angular rate to the wind speed has an upper yield point. Therefore, we need to investigate Marimo's rotational angular rate by conducting more field observations. Additionally, other methods, like laboratory experiments, are necessary to clarify the relationship between wind waves and Marimo's rotational angular rate.

The monthly mean rotational angle was estimated by using wind data sets from June to October in 2014 and 2015 (Figs. 4b, 11). Then, the average rotational angular rate was modelled as a function of wind speed, $r^2=0.65$ ($p<0.01$; a Shapiro-Wilk normality test and a Pearson correlation test using a statistical software R (ver.3.1.0) (Fig. 4a). The monthly mean rotational angle was largest in June and smallest in October. Consequently, the Marimo oscillate and rotate from June to October when the water surface is free from ice cover. Thus, the Marimo are polished due to the oscillation and rotation, enabling a highly dense surface of green alga filaments to form, and fixed into a ball by the rocking motion. On the other hand, since Lake Akan is covered by ice from December to April, the Marimo are in a hibernation-like state over this period due to low water temperature. As there is no external force to oscillate and rotate the Marimo, they do not become polished, suggesting that the surface density of green alga filaments becomes lower during the ice-cover period^{23,29}. Thus, we conjecture that Marimo develop a sparse cover of green alga filaments each winter followed by a dense cover in summer, resulting in annual rings. As suggested above, the predominant thickness of the annual rings, composing Marimo, is 6.3 mm and 4.5 mm, using the spectrum's first and second peaks. Therefore, the regions of alternately sparse and dense green alga filaments enable us to estimate the Marimo's diameter growth rate, 12.6 mm/year or 9.0 mm/year. Here, we summarize the results as follows:

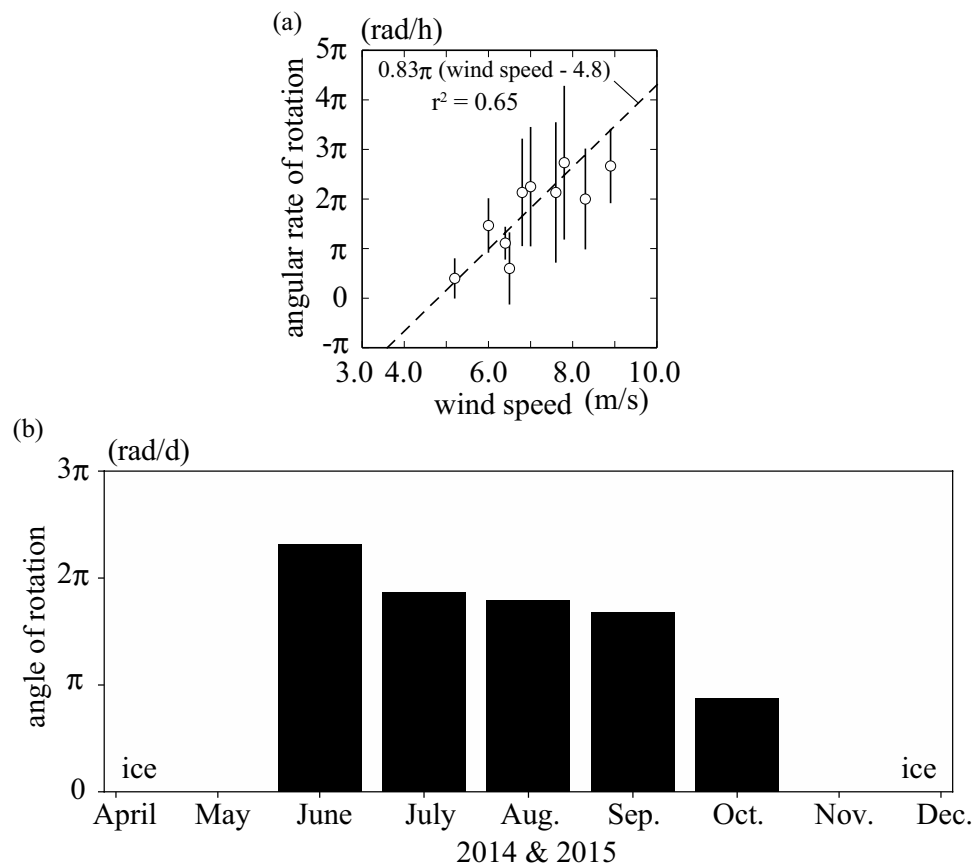


Figure 4. Wind and rotation of Marimo. (a) Wind speed and average angular rate of the rotation of Marimo. Solid lines indicate the standard deviation of average angular rate (average \pm SD (n=3-10)). (b) The diurnal angle of the rotation of Marimo in 2014 and 2015.

- (1) Inflow does not affect Marimo motion on regular days. In contrast, the strong wind, such as by typhoon, causes wind-driven current but not significant oscillational flow, resulting in that Marimo are washed from the colony to shore.
- (2) The fetch is a significant factor controlling wind waves in the Marimo colony, polishing the Marimo surface during no ice period^{5,24,25}.
- (3) Our field observations revealed that land and sea breeze frequently occurs at Churui Bay, providing enough oscillational motion to Marimo during no ice period.
- (4) Marimo surface becomes bushy with no motion during the ice-cover period²⁹.
- (5) During the ice-cover period, the water surface is covered entirely in Lake Akan, and the fetch becomes zero, meaning that there is no Marimo movement.
- (6) The MRI analysis revealed that the Marimo sampled in June and July have lower void ratio adjacent to the surface of Marimo than a few mm inside. Therefore, the sparse and dense patterns correspond to the annual growth rate of Marimo, suggesting that the Marimo's diameter growth rate may be 12.6 mm/year or 9.0 mm/year.

Self-sustained growth of Marimo. MRI analysis and field observations showed that the oscillation and rotation of Marimo due to wind waves polished and increased the density of green alga filaments at the surface of Marimo from June to October. In contrast, the void ratio became higher adjacent to the Marimo surface from December to April because the water surface was covered by ice, and there was no external force (Fig. 5a,b). In addition, the predominant growth rate in the diameter of Marimo was revealed to be 12.6 mm/year. Hence, it takes 17 years for Marimo to grow in diameter from 3 to 25 cm. In the event of a typhoon, strong winds often wash giant Marimo from a colony to shore. The giant Marimo in the shore collapse to the smaller size, tumble down over the sloping lake bottom and fall to lower layers in the colony (Fig. 5c). According to the Marimo Conservation Council¹⁹, such "generational change" occurs every 5 to 9 years¹⁹. The larger the diameter of the individual Marimo, the more likely it will be to lie on the colony's top layer. Since the occurrence cycle of most typhoons is shorter than the growth period of giant Marimo, generational change is one of the most significant factors controlling the formation of giant Marimo.

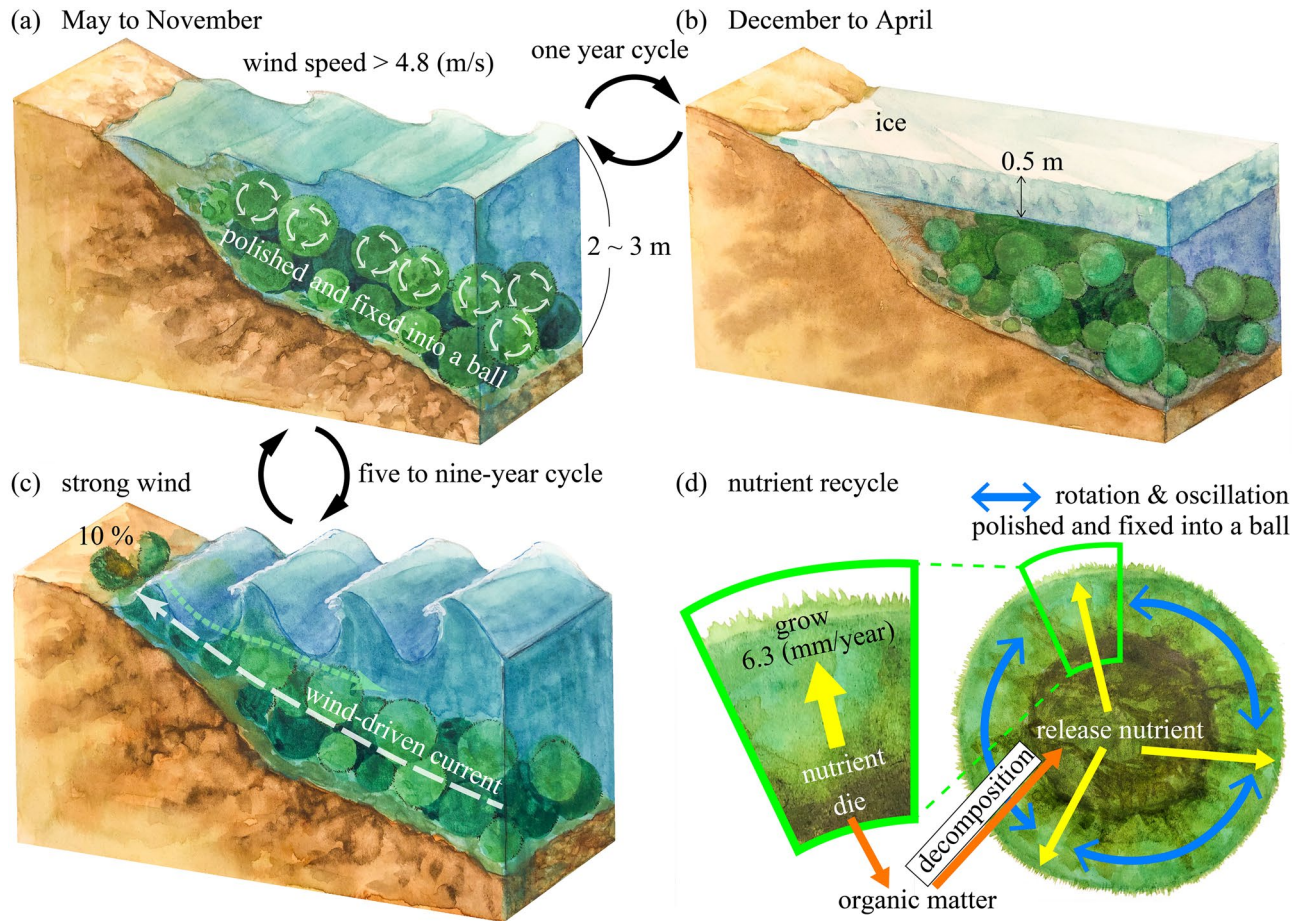


Figure 5. Formation of giant Marimo. **(a)** Growth period: June to October. **(b)** Hibernation period: November to May. **(c)** Marimo are washed ashore due to strong wind, and a small-size Marimo goes back to the Marimo colony. **(d)** Nutrient recycling in Marimo. Illustration adapted with permission from Reina Nakayama.

We conducted field observations to investigate the water quality inside and outside the Marimo by sampling 12 samples in June and August of 2015. The mean DO concentration in the Marimo interior was 7.8 mg/L with a mean water temperature of 11.5 °C in June. Also, the interior DO concentration was 2.3 mg/L with a mean water temperature of 27.5 °C in August, one of the hottest months in Lake Akan, but the interior water was not anoxic. Because the DO concentrations on the Marimo exterior in June and August were 10.5 mg/L and 8.7 mg/L, respectively, we anticipated that the water exchange might inhibit the occurrence of anoxia in the central cavity. We carried out laboratory experiments to evaluate the DO consumption rate of the interior water and then estimated the residence time of the interior water. The mean DO consumption rates in June and August were 0.67 mg/L/d and 1.9 mg/L/d, respectively. The mean residence time was found to be 105 h. On the other hand, detached organic matter decomposes in the Marimo interior, causing nutrients to be released, and thus we also measured total dissolved nitrogen (TDN) of 0.093 mg/L and total dissolved phosphorus (TDP) of 0.012 mg/L in the Marimo interior, which corresponded to the estimates in a previous study³⁰. The exterior water's TDN and TDP were 0.008 mg/L and 0.005 mg/L, and Churui Bay is categorized as being in an oligotrophic state. The TDN/TDP values were 7.6 and 1.6 inside and outside Marimo, suggesting that high nutrients are released, condensed, and used to grow selectively. Therefore, the oscillation and rotation of Marimo play a significant role not only in polishing the Marimo and fixing it into a ball (Fig. 5a) but also in reusing the high levels of nutrients recycled inside the Marimo for growth (Fig. 5d).

Conclusion

This study showed that a single organism, *A. linnaei*, existing in its aggregated form as a Marimo, is sustained by the world smallest nutrient recycling system, which is controlled by the oscillation and rotation of the Marimo due to wind waves. Namely, mortality, decomposition and mineralization managed by the oscillation and rotation of the Marimo enable the condensing of nutrients in the Marimo interior with an adequate balance of nitrogen/phosphorous. Thus, Marimo's green alga filaments grow by consuming oligotrophic nutrient on their exterior surfaces and by consuming high levels of nutrients recycled from the detached organic matter in the Marimo interior. The nutrient recycling system, which may be the world's smallest nutrient cycle, supported by the decomposition and mineralization of organic matter, is similar to the nutrient cycle in Shiretoko, the World Natural Heritage, in which salmon return to the rivers for spawning and transport nutrients from the ocean to

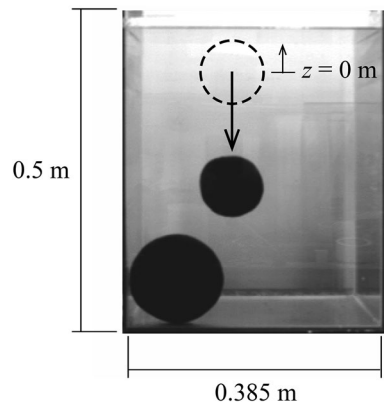


Figure 6. Underwater drop test of a Marimo to estimate its drag coefficient.

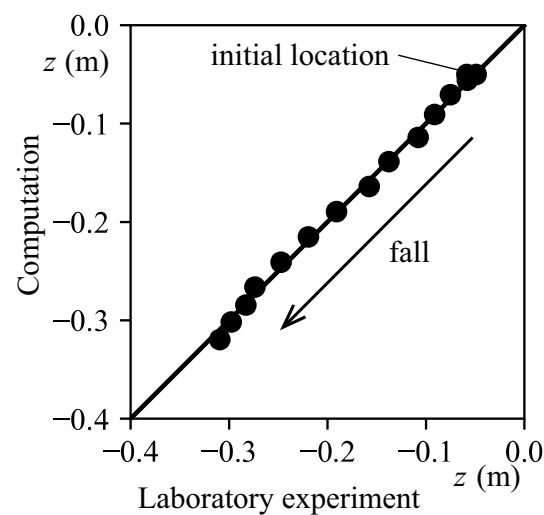


Figure 7. An example of an underwater drop test. Comparison of drop locations between the laboratory experiment and computation. The water surface corresponds to $z = 0$ m.

the inland waters³¹. The nutrient cycle is one of the most important mechanisms to support an ecosystem in an oligotrophic natural environment. Unfortunately, the nutrient cycles of Marimo and other organisms might be in danger due to climate change. In Churui Bay, climate change may vary the mean wind speed and the frequency of strong wind, which would deteriorate the water exchange between the Marimo interior and exterior and the Marimo's growth rate. Since the self-sustained growth of Marimo is achieved by balancing the growth rate and generational change, the loss of an appropriate physical environment may cause irreversible degradation in the ecosystem for Marimo.

Methods

The underwater specific density of Marimo. We conducted an underwater drop test using laboratory experiments and field observations to estimate Marimo's specific density ($\varepsilon = (\rho_m - \rho_w)/\rho_m$, ρ_m : the density of Marimo, ρ_w : the density of water). First, as the drag coefficient of Marimo is unknown, we carried out an underwater drop test using a water tank (Fig. 6). We used a water tank of 38.5 cm in width, 38.5 cm in length and 50.0 cm in height for the laboratory experiments. A high-speed camera with a frame rate of 125 s^{-1} was used to capture the central location of Marimo (Fig. 7). The drag coefficient of Marimo was revealed to be the same as a sphere, $C_D = 0.42$. Then, we conducted an underwater drop test in Churui Bay using 56 real Marimo on the 15th of June and 21st of August of 2015 (Fig. 8). To estimate the specific density of Marimo, we applied the vertical momentum equation, which revealed that the larger the Marimo's diameter, the smaller the Marimo's specific density:

$$V_m \frac{\partial u_m}{\partial t} = -\varepsilon g V_m - C_D A_m |u_m| u_m,$$

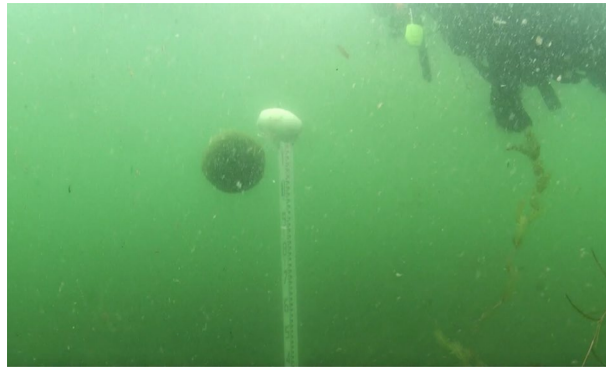


Figure 8. Field observation for estimating the underwater specific density of Marimo at Churui Bay in Lake Akan.

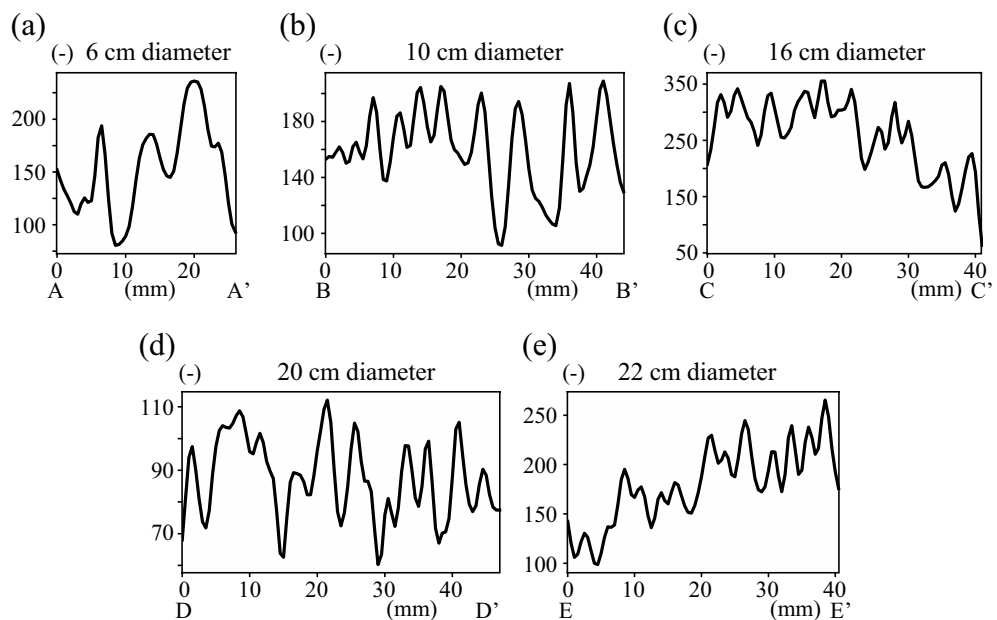


Figure 9. MRI values in Fig. 3. (a) A–A', (b) B–B', (c) C–C', (d) D–D', (e) E–E'.

where eV_m is the volume of Marimo ($= 4\pi r_m^3/3$) (m^3), r_m is the radius of Marimo, u_m is the vertical moving speed of Marimo (m/s), ε is the underwater specific density of Marimo ($\varepsilon = (\rho_m - \rho_w)/\rho_m$), ρ_m is the density of Marimo (kg/m^3), ρ_w is the density of water (kg/m^3), C_D is the drag coefficient of Marimo, and A_m is the projected area of Marimo ($= \pi r_m^2$) (m^2).

Magnetic resonance image analysis. We obtained a proton density-weighted image using Head Coil, which showed that the higher the density of green alga filaments, the larger the MRI value. Coronal images were obtained, and the conditions were TR/TE = 2700 ms/15 ms, TI (inversion time) = 1100 ms, NEX 2, acquisition matrix = 256×255 , field of view = $256 \text{ mm} \times 256 \text{ mm}$, slice thickness = 4 mm, and image matrix = 512×512 . MRI values along the lines of A–A', B–B', C–C', D–D' and E–E' in Fig. 3 are plotted in Fig. 9. The surface thickness is more than 4 cm and close to 5 cm in the Marimo of diameter 10 cm (B–B') and 20 cm (D–D'), and the sparse and dense green alga filament thickness ranges from 4 to 8 mm (Fig. 9b,d). In contrast, the minimum sparse and dense thickness is about 2 mm in the Marimo of diameter 22 cm (E–E'), but the dominant sparse and dense thickness is about 5 to 6 mm. The spectrum using all MRI values along the normal direction was obtained to investigate the predominant thickness of the annual rings (Fig. 9). In the spectrum analysis, all MRI values were connected into one continuous data after removing the trend. The spectrum analysis showed that the first peak growth rate was 12.6 mm/year, and the second peak growth rate was 9.0 mm/year. Figure 9 suggests that the growth rate of Marimo varies by the growth stage, environmental conditions, etc. It will be necessary to investigate the growth rate of Marimo in greater detail in a future study.

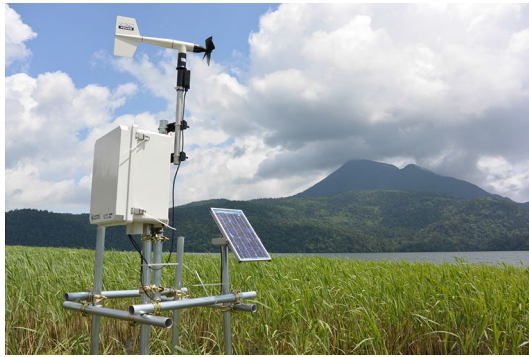


Figure 10. Meteorological station for measuring wind speed and direction at Churui Bay in Lake Akan.

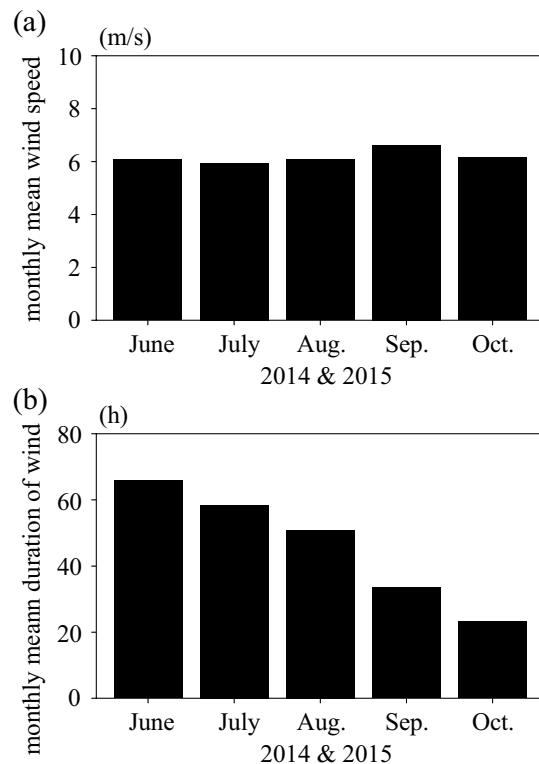


Figure 11. Wind speed and rotation of Marimo. (a) Monthly mean wind speed at Churui Bay in Lake Akan in 2014 and 2015. (b) Monthly mean duration of wind more than 4.8 m/s at Churui Bay in Lake Akan in 2014 and 2015.

Wind speed and direction. Wind speed and direction were measured at 2 m above the water surface in Churui Bay from the 3rd of July to the 5th of November in 2014 and from the 11th of June to the 11th of August in 2015 (R. M. Young Company, Wind Monitor Model 05103) (Fig. 10). We applied the log law using the lake surface roughness to estimate wind speed at 10 m above the water surface. The roughness was 0.0001 m, and the wind speed at 10 m was 1.16 times greater than that at 2 m. Marimo moves predominantly when the wind direction is from the southeast to the southwest. The monthly mean wind speed was almost constant, about 6.0 m/s, from June to October in 2014 and 2015 (Fig. 11a). In contrast, the monthly mean duration of wind in June was the most prolonged, 60 h, and that in October was the shortest, 20 h (Fig. 11b). Significantly, Marimo showed the highest rate of oscillations and rotations soon after the ice at the water surface was melted. Note that the wind duration was summed up when wind speed was more than 4.8 m/s.

Wave height and period. We conducted field observations to measure significant wave height and period at Churui Bay using a Wave Hunter set up at a water depth of 3 m (WH-503; I.O. Technique Co.). Wind waves

were measured with an interval of 20 min from the 15th of July to the 14th of September in 2014, with an interval of 2 h from the 14th of September to the 5th of November in 2014, and with an interval of 2 h from the 8th of June to the 11th of August in 2015. Wilson's formulas were used to model significant wave height and period, which agreed well with the field observations. The appropriate wind duration was 30 min, and the 30 min mean significant wave height and period were used in the validation. The best fit fetch was from 2.0 to 2.5 km for Wilson's formulas³²:

$$\frac{gH_{1/3}}{U^2} = 0.30 \left[1 - \frac{1}{\left\{ 1 + 0.004 \left(\frac{gF}{U^2} \right)^{1/2} \right\}^2} \right],$$

$$\frac{gT_{1/3}}{2\pi U} = 1.37 \left[1 - \frac{1}{\left\{ 1 + 0.008 \left(\frac{gF}{U^2} \right)^{1/3} \right\}^5} \right],$$

where $H_{1/3}$ is the significant wave height (m), $T_{1/3}$ is the significant wave period (s), U is the wind speed (m s^{-1}), F is the fetch (m), and g is the gravity acceleration (m s^{-2}).

Dissolved oxygen and consumption rate of dissolved oxygen inside of Marimo. We sampled the water inside Marimo using a syringe with a needle of diameter 0.69 mm and length 15 cm on the 9th of June and the 11th of August in 2015. Six syringe samples were collected for each Marimo to sample about 300 mL. Dissolved oxygen was measured using two portable water quality sensors (nos. HQ30d from Hach and 8,506,300 from Luminescent DO Sensor). The dissolved oxygen consumption rate was estimated by giving the initially saturated dissolved oxygen under constant water temperature conditions. Dissolved oxygen was measured every 3 h for 2 days. As a result, we obtained the following Arrhenius equation:

$$SOD = 1.02 \times 10^8 \exp \left[\frac{-7.43 \times 10^{-20}}{1.380649 \times 10^{-23} (273.15 + T_w)} \right],$$

where T_w is the water temperature ($^{\circ}\text{C}$).

We estimated the inside water's residence time using the following equation:

$$T_R = \frac{DO_{out} - DO_{in}}{SOD},$$

where T_R is the residual time inside the Marimo (h), DO_{out} is the DO around the Marimo (mg/L), DO_{in} is the DO inside the Marimo (mg/L), and SOD is the DO consumption rate inside the Marimo (mg/L/h).

Nutrients. A diver sampled water inside the Marimo on the 31st of August in 2017; the same water sample was used for the dissolved oxygen measurement. 300 mL of water from the interior of the Marimo was collected, and the samples were brought to the laboratory in a cool box within a few hours. Water was filtered using a hydrophobic PTFE disposable membrane filter (DISMIC 25HP020AN; ADVANTEC), and TDN and TDP were measured using an autoanalyzer (QuAAtro 2HR; BLTEC).

Data availability

The data that support the findings of this study are available from the corresponding author upon reasonable request.

Received: 28 July 2021; Accepted: 21 October 2021

Published online: 10 November 2021

References

- Boedeker, C., Eggert, A., Immers, A. & Wakana, I. Biogeography of *Aegagropila linnaei* (Cladophorophyceae, Chlorophyta): A widespread freshwater alga with low effective dispersal potential shows a glacial imprint in its distribution. *J. Biogeogr.* **37**, 1491–1503 (2010).
- Boedeker, C. & Sviridenko, B. F. *Cladophora koktschetavensis* from Kazakhstan is a synonym of *Aegagropila linnaei* (Cladophorales, Chlorophyta) and fills the gap in the disjunct distribution of a widespread genotype. *Aquat. Bot.* **101**, 64–68 (2012).
- Brand, F. Die *Cladophora-Aegagropilen* des Süßwassers. *Hedwigia* **41**, 34–71 (1902).
- Kurogi, M. Lake ball 'Marimo' in Lake Akan. *Jpn. J. Phycol.* **28**, 168–169 (1980).
- Van den Hoek, C. *Revision of the European Species of Cladophora* (E. J. Brill, 1963).
- Pankow, H. *Aegagropila sauteri* in Mecklenburg (Norddeutschland). *Nova Hedwigia* **9**, 177–184 (1965).
- Einarsson, A. *et al.* The ecology of Lake Myvatn and the River Laxá: Variation in space and time. *Aquat. Ecol.* **38**(2), 317–348. <https://doi.org/10.1023/b:aeco.0000032090.72702.a9> (2004).
- Wakana, I., Satoh, H. & Suzuki, Y. The past and the present of vegetation and environment in a disappeared habitat of the freshwater alga Marimo (*Aegagropila linnaei*) in Lake Akan. *Jpn. J. Plant Res.* **119**(Suppl.), 63 (2006).
- Boedeker, C. & Immers, A. No more lake balls (*Aegagropila linnaei* Kützinger, Cladophorophyceae, Chlorophyta) in The Netherlands?. *Aquat. Ecol.* **43**, 891–902 (2009).

10. Boedeker, C., Anja, E., Anne, I. & Erik, S. Global decline of and threats to *Aegagropila linnaei*, with special reference to the lake ball habit. *Bioscience* **60**(3), 187–198. <https://doi.org/10.1525/bio.2010.60.3.5> (2010).
11. Einarsson A. The lake balls of Mývatn in memoriam. Mývatn Research Station, https://www.ramy.is/wordpress/wp-content/uploads/2014/05/Lake_Ball_in_memoriam_final_draft_reduced_size.pdf Iceland (2014).
12. Wesenberg-Lund, C. Sur les Aegagropila sauteri du Lac de Soro. *Acadé 'mie Royale des Sciences et des Lettres de Danemark* **2**, 167–203 (1903).
13. Niiyama, Y. Morphology and classification of *Cladophora aegagropila* (L.) Rabenhorst in Japanese lakes. *Phycologia* **28**, 70–76 (1989).
14. Nakayama, K. *et al.* Investigation of wind waves which induce rotational motion of Marimo in Lake Akan. *J. JSCE Ser. B3 (Ocean Eng.)* **71**(2), I_945-I_950 (2015) (in Japanese with English abstract).
15. Kurogi, M. in *The Growing Condition and Habitat Environment of Marimo in Lake Akan, a Special Natural Monument of Japan* (ed. Kurogi M.) 80–87 (Akan Town, 1976) (in Japanese).
16. Tatewaki, M. in *Report of Marimo Survey in FY 1950–1951* (ed. Tatewaki, M.) 1–56 (Expert Committee of Marimo, 1952) (in Japanese).
17. Kurogi, M. (ed.) *Annual Report FY 1985–1986 "the Growing Condition of Marimo in Lake Akan, a Special Natural Monument of Japan"* (Akan Town, 1986) (in Japanese).
18. Akan Town Board of Education (ed.) Abridged edition of the report of the 3rd research project of 'Marimo', a special natural monument of Japan. *Marimo Research, Special Issue 1–46* (1998) (in Japanese).
19. Marimo Conservation Council (ed.) *The Marimo Protection and Management Plan*. (Marimo Conservation Council, 2012) (in Japanese).
20. Soejima, A., Yamazaki, N., Nishino, T. & Wakana, I. Genetic variation and structure of the endangered freshwater benthic alga Marimo, *Aegagropila linnaei* (Ulvophyceae) in Japanese lakes. *Aquat. Ecol.* **43**(2), 359–370 (2009).
21. Boedeker, C. The attached form of the endangered freshwater alga *Aegagropila linnaei* Kützting (Chlorophyta) is found in the Zuideindigerwiede, The Netherlands. *Aquat. Bot.* **92**, 75–77 (2010).
22. Lorenz J. R. *Die Stratonomie von Aegagropila sauteri*. 147–172 (*Denkschr. Akad. Wiss. Wien* **10**, 1856) (in Germany).
23. Kanno, R. A study of *Aegagropila* of Japan, with special reference to the ball formation. *Bull. JSFS* **2**(5), 217–228 (1934) (in Japanese with English abstract).
24. Fukutomi, T., Kusunoki, K. & Tabata, T. in *Report of Marimo Survey in FY 1950–1951* (ed. Tatewaki, M.) 67–101 (Expert Committee of Marimo, 1952) (in Japanese).
25. Sano, F. *et al.* Projection of wind waves which induce rotational motion of Marimo in Lake Akan. *J. JSCE Ser. B3 (Ocean Eng.)* **72**(2), I_988-I_993 (2016) (in Japanese with English abstract).
26. Togashi, T., Sasaki, H. & Yoshimura, J. A. Geometrical approach explains LakeBall (Marimo) formations in the greenalga, *Aegagropila linnaei*. *Sci. Rep.* **4**, 3761. <https://doi.org/10.1038/srep03761> (2014).
27. Hayashi, N., Nakayama, K., Oyama, Y., Yamada, T. & Komai, K. Estimation of rotation angle and critical velocity of Marimo due to waves and currents. *J. JSCE Ser. B1 Hydr. Eng.* **75**(5), I_769-I_774 (2019) (in Japanese with English abstract).
28. Phillips, N., Draper, T. C., Mayne, R. & Adamatzky, Z. Marimo machines: Oscillators, biosensors and actuators. *J. Biol. Eng.* **13**, 72. <https://doi.org/10.1186/s13036-019-0200-5> (2019).
29. Yamada, Y. & Sakai, Y. A study for forming spherical aggregations of Marimo. *Bull. Jpn. Soc. Phycol.* **9**(2), 73–75 (1961) (in Japanese).
30. Nakazawa, S. *Why Marimo Has the Spherical Shape: Its Ecology and Morphology* (Chuokoronsha, 1989) (in Japanese).
31. Nakayama, K., Maruya, Y., Matsumoto, K., Komai, K. & Kuwae, T. Nitrogen fluxes between the ocean and a river basin using stable isotope analysis. *Estuar. Coast. Shelf Sci.* **212**, 286–293. <https://doi.org/10.1016/j.ecss.2018.07.015> (2018).
32. Wilson, B. W. Numerical prediction of ocean waves in the North Atlantic for December, 1959. *Dtsch. Hydrogr. Z.* **18**(3), 114–130 (1965).

Acknowledgements

This work was supported by the Japan Society for the Promotion of Science (Grant No. 18H01545). We thank D. Kokuryo, K. Kyotani, K. Iwata, T. Ohji and I. Wakana for committing their time to this research. We owe a special thanks to R. Nakayama for constructing the figures.

Author contributions

K.N. designed the field experiments and laboratory experiments, wrote most of the paper, and performed all analysis. K.K., T.Y., Y.S., F.S. and Y.O. carried out the field experiments and analyzed the effect of wind-wave on the formation of giant Marimo. K.O., S.H., Y.S. and E.K. carried out the laboratory experiments using magnetic resonance image analysis. All authors read and commented on drafts of this paper.

Competing interests

The authors declare no competing interests.

Additional information

Correspondence and requests for materials should be addressed to K.N.

Reprints and permissions information is available at www.nature.com/reprints.

Publisher's note Springer Nature remains neutral with regard to jurisdictional claims in published maps and institutional affiliations.



Open Access This article is licensed under a Creative Commons Attribution 4.0 International License, which permits use, sharing, adaptation, distribution and reproduction in any medium or format, as long as you give appropriate credit to the original author(s) and the source, provide a link to the Creative Commons licence, and indicate if changes were made. The images or other third party material in this article are included in the article's Creative Commons licence, unless indicated otherwise in a credit line to the material. If material is not included in the article's Creative Commons licence and your intended use is not permitted by statutory regulation or exceeds the permitted use, you will need to obtain permission directly from the copyright holder. To view a copy of this licence, visit <http://creativecommons.org/licenses/by/4.0/>.

© The Author(s) 2021